14TH EUROPEAN CONFERENCE ON COMPOSITE MATERIALS
7-10 June 2010, Budapest, Hungary
Paper ID: 065-ECCM14

TOWARDS A PROCESS SIMULATION TOOL FOR THE LASER ASSISTED TAPE PLACEMENT PROCESS

W. J. B. Grouve[1*], L.L. Warnet[1], R. Akkerman[1]

[1]*University of Twente, Faculty of Engineering Technology, the Netherlands*
**corresponding author email: W.J.B.Grouve@utwente.nl*

Abstract

A combined optical and thermal model for the laser assisted tape placement process is presented. The optical model adopts a ray tracing procedure, based on the Fresnel equations, to predict the incident heat flux on the tape and substrate near the nip-point. The heat flux distribution is subsequently used in a one-dimensional thermal model to predict the temperature distribution in the tape and substrate. The results demonstrate that for small incident laser angles a part of the laser light is reflected at the surface, which significantly influences the temperature distribution in the nip-point. The presented model allows, with a weld strength and consolidation model, optimization of the processing parameters.

1 Introduction

The laser assisted tape placement process involves welding of fibre reinforced thermoplastic tapes onto a pre-consolidated substrate. The substrate is manufactured by either conventional technologies, such as autoclave processing, or by the tape placement process itself. The final product properties can be tailored to a high degree by incrementally adding tapes on predefined paths in the desired orientation. The process potentially allows for 'out-of-autoclave' production which, combined with the high degree of automation by using industrial robots [1,2], makes the process attractive for the aerospace industry.

The thermal and pressure history of the tape and substrate govern the final product properties [3,4,5]. The process window is often narrow [6] and has to be chosen carefully in order for this tape placement process to compete with conventional production technologies such as autoclave processing. Currently, this process window is determined to a large extent by trial and error procedures involving extensive and laborious material inspection. The development of predictive process simulation tools, to define the process window, could help evolve the laser assisted tape placement process into a true 'out-of-autoclave' technology.

The current paper presents a combined optical and thermal model to predict the temperature distribution during the process. A bond strength development or consolidation model can be added, as shown in Figure 1, to study the influence of processing parameters on product performance. The optical model adopts a ray tracing procedure to predict the incident laser

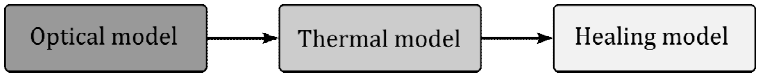

Figure 1 Modelling approach.

heat flux distribution on the tape and substrate near the nip-point. The calculated heat flux is subsequently used in a one-dimensional transient heat transfer model to calculate the temperature distribution in the tape tape and substrate.

The next section provides a description of the laser assisted tape placement process together with a brief overview of available modelling approaches in literature. Section three describes the optical and thermal model. Subsequently the influence of incident laser angle and placement velocity on the temperature distribution in the tape and substrate is investigated. Finally, the conclusions and future work are presented.

2 The laser assisted tape placement process

Figure 2 schematically illustrates the laser assisted tape placement process. A unidirectional fibre reinforced tape is guided between a compaction roller and a substrate. The tooling which supports the substrate can be doubly curved, allowing the production of complex parts. A laser source heats the incoming tape and substrate, while the compaction roller moves forward on a predefined path. The thermoplastic fibre reinforced tapes are welded onto the substrate under the application of heat and pressure. The bond strength strongly depends on the complex thermal and pressure history of the interface between tape and substrate [7]. The tape and substrate are subjected to high heating and cooling rates, while pressure is applied momentarily. Furthermore, thermal residual stresses might develop during the process and deteriorate product performance [8]. The degree of crystallinity, in case of semi-crystalline matrix materials, is also affected by the thermal history [4].

The heat transfer models found in literature reflect the pronounced role of temperature in the tape placement or tape winding process. The majority of available models concern the case in which heat is applied using a hot gas torch. Different solution methodologies are pursued ranging from relatively simple one-dimensional [5] or two- dimensional [9] approaches to more complex three-dimensional transient FE models [10,11].

Only a few models concern the application of a laser to heat the tape and substrate. Beyeler and Güçeri [12] adopted a two dimensional finite difference method to calculate the temperature distribution during the process. The laser light is assumed to be absorbed entirely by the tape and substrate material and the possible reflection of laser light is neglected. Grove [13] predicted the temperature using a two-dimensional finite element model. The reflection of the laser light was taken into account by assuming a constant reflectivity, independent of the angle of incidence, for the tape and substrate surface.

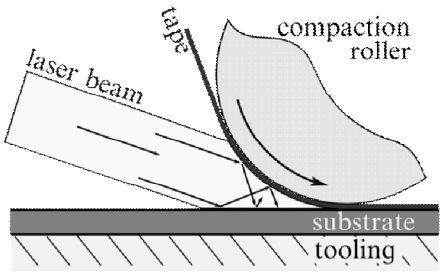

Figure 2 Schematic representation of the laser assisted tape placement process.

The current paper presents a ray tracing model to predict the incident heat flux distribution on the tape and substrate near the nip-point. The calculated heat flux distribution is subsequently used in a one-dimensional thermal model to predict the temperature distribution in the tape and substrate during the process. The heat equation is solved using a pseudospectral, or collocation, method to account for the high temperature gradients in the substrate and tape.

3 Process model

This section presents the optical and thermal models which will, when combined with a bonding and consolidation model, serve as a process design tool. The optical model predicts the incident heat flux distribution on the tape and the substrate. The heat flux distribution serves as an input to the thermal model, which calculates the temperature in the tape and substrate. Currently, there is no effect of the thermal model on the optical model taken into account, although strictly, the refractive indices of the tape and laminate depend on temperature.

3.1 Optical model: incident heat flux

The spatial distribution of incident laser heat flux influences the temperature distribution in the tape and substrate and subsequently the temperature history at the interface between substrate and tape. The incident laser light is partly reflected by the tape and substrate surface, during the process. Although the geometry of the nip-point ensures that all light is ultimately absorbed by the tape and substrate, detailed calculation is necessary to determine the actual spatial distribution. A geometrical model of the nip-point is developed for this purpose and a ray tracing procedure is followed to calculate the heat flux distribution.

When light strikes a surface it partly reflects according to the law of reflection, which states that the angle of reflection φ_r equals the angle of incidence φ_i, as shown in Figure 3. A part of the incident intensity I_0 is reflected I_r, while the remaining part is either absorbed I_a or transmitted I_t. It is assumed that virtually no laser light is transmitted in the case of carbon reinforced tapes. It is therefore adequate to write:

$$A = 1 - R \tag{1}$$

where R is the fraction of reflected light (I_r/I_0), known as reflectance, and A is the fraction of absorbed intensity (I_a/I_0), which is known as the absorbance. The intensity of the reflected light is calculated using the Fresnel equations. The reflectance R depends on the polarization

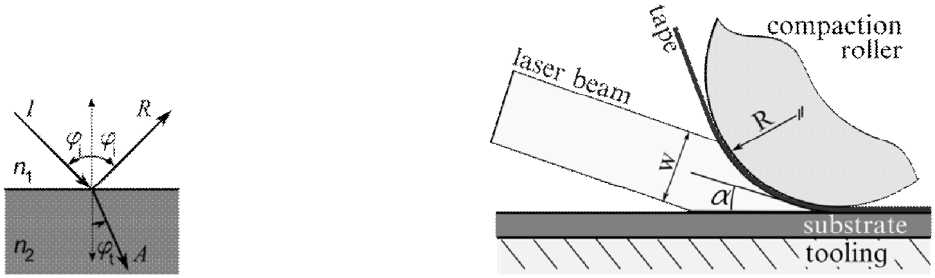

Figure 3 Variables used in the Fresnel equations and Snell's law.

of the incident light with respect to the surface. The reflectance for s- and p-polarized light with respect to the surface yields:

$$R_s = \left[\frac{\sin(\varphi_t - \varphi_i)}{\sin(\varphi_t + \varphi_i)}\right]^2 \quad \text{and} \quad R_p = \left[\frac{\tan(\varphi_t - \varphi_i)}{\tan(\varphi_t + \varphi_i)}\right]^2 \tag{2}$$

The angle of incidence φ_i is defined with respect to the normal of the surface, while the angle of refraction φ_t can be calculated using Snell's law:

$$\frac{\sin\varphi_i}{\sin\varphi_t} = \frac{n_1}{n_2} \tag{3}$$

in which n_1 and n_2 represent the refractive indices of the two media, as shown in Figure 3. It is assumed that the laser light is unpolarized, that is the light contains an equal amount of s- and p-polarized light:

$$R = (R_s + R_p)/2 \tag{4}$$

The nip-point geometry shown in Figure 3 consists of a substrate, a tape conforming the compaction roller and a laser source. The laser beam has a width w of 30 mm. Table 1 lists the values for the parameters used in the simulations. In the present analysis the midline of the laser beam is aimed at the nip-point. For sake of simplicity the refractive index is chosen equal to 1.5, which corresponds to a value in the range of most thermoplastics at room temperature. Strictly, the refractive index depends on the wavelength of the light and temperature. These two factors, as well as the inhomogeneous nature of the tape, are not accounted for.

An array of light sources is generated at the laser source location, assuming uniform intensity. A ray tracing methodology is adopted, following each light ray. The angle of reflection φ_r and reflectance R are calculated using Equation (2), (3) and (4), when the ray hits the tape or substrate surface. The incident heat flux is determined using Equation (1) and the incident angle φ_i. The ray is followed until it leaves the nip-point region or in case the intensity drops below a pre-set threshold value, which is set to 2% of the original intensity for the present analysis.

Figure 4 shows the normalised incident heat flux on both tape and substrate as a function of the distance from the nip-point for an arbitrary laser angle α of 22°. The figure shows the contribution of the laser light which comes directly from the source as well as the light which

Parameter	Value
beam width w, mm	30
compaction roller radius R, mm	40
refractive index tape and substrate n_2, -	1.5
refractive index air n_1, -	1.0

Table 1 Geometric and optical properties used in the ray tracing model.

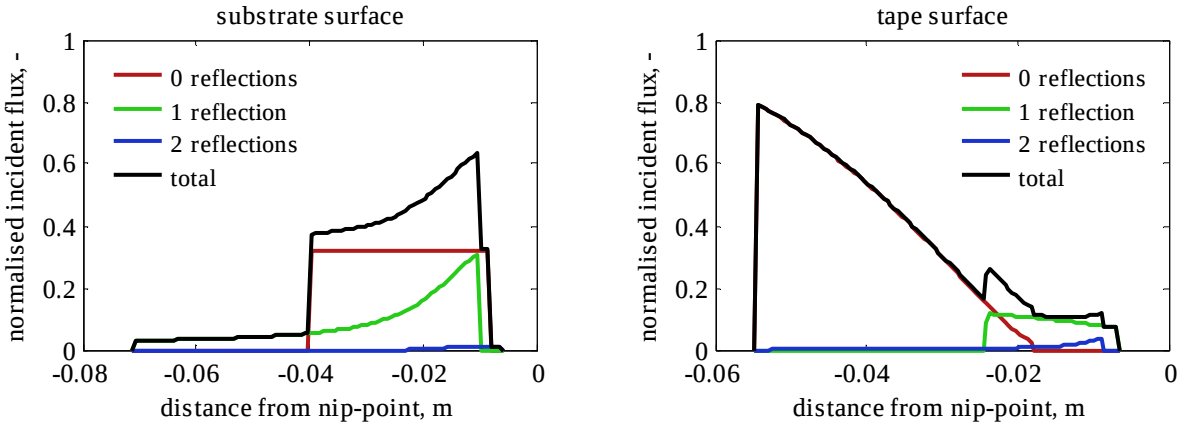

Figure 4 Incident heat flux distribution on the substrate and tape as a function of the distance from the nip-point for a laser angle α of 22°.

has reflected on the tape or surface. The intensity of the light proves to be negligible after the two reflections, which is shown by the blue lines in Figure 4. Both figures show that, with the current configuration, no light is able to penetrate deeply into the nip-point. The incident flux on the substrate decreases fast near the nip-point due to the shadowing effect of the roller. The tape influx decreases as the tape bends away from the source reducing the angle of incidence. The obtained heat flux distribution will serve as an input for the thermal model, which is introduced in the following section.

3.2 Thermal analysis

3.2.1 Thermal model

A thermal model was developed to calculate the substrate and tape temperature during processing. The tape and substrate are treated separately before the nip-point and are coupled thereafter. An approach is followed similar to the one adopted by Thierney and Gillespie Jr. [5]. The through-the-thickness heat conduction is assumed to dominate the thermal problem. The in-plane heat conduction is therefore neglected. A one-dimensional Lagrangian approach is adopted in which a through thickness slice of material (tape or substrate) is followed in time. The temperature distribution is described by the one dimensional energy balance:

$$\rho c_p \frac{\partial T}{\partial t} = k_z \frac{\partial^2 T}{\partial z^2} \tag{5}$$

in which ρ is the density, c_p the specific heat and k_z the through thickness heat conductivity.

The effect of crystallization heat is neglected [14]. The material properties of APC-2 carbon/PEEK [4] are used and listed in Table 2. The energy balance is solved for the tape, substrate and coupled domain.

3.2.2 Boundary and initial conditions

The tape, substrate and coupled domain are subjected to the following boundary conditions:

$$k_z \frac{\partial T}{\partial z} = -h_{air}(T - T_{far}) + Q_{in}(t), \quad \text{on heated surface} \tag{6}$$

$$k_z \frac{\partial T}{\partial z} = -h_{tool}(T - T_{far}), \quad \text{on tooling surface} \tag{7}$$

where $Q_{in}(t)$ is the incident heat flux by the laser on the surface calculated using the ray-tracing procedure, explained in the previous section. The coupled domain, after the nip-point, is not heated by the laser and therefore the incident heat flux equals zero. The heat transfer coefficient of the air and tooling, i.e. the compaction roller and the steel mould respectively, are listed in Table 2 [15]. Heat transfer due to radiation is neglected in the present analysis. Initially the tape and substrate temperature equal the ambient temperature:

$$T(z,0) = T_{initial} \tag{8}$$

After the nip-point the two domains are coupled at the interface. The initial through thickness temperature distribution for the coupled domain follows directly from the tape and substrate temperature distribution at the nip-point.

3.2.3 Computational procedure

The heat transfer equation, Equation (5), is discretized in space and time and subsequently solved to obtain the temperature distribution after the nip-point. A pseudospectral, or collocation, method is applied to discretize the equation in space in order to accurately describe the high temperature gradients in the substrate and tape. The solution in the spatial domain is approximated by a polynomial function of order N, which was greater than 16 in the present analysis:

$$T(z) = \sum_{i=1}^{N} T_i L_i(z) \tag{9}$$

in which T_i is the temperature at collocation point i and $L_i(z)$ is a Lagrange polynomial, defined as:

$$L_i(z) = \prod_{j=1, j \neq i}^{N} \frac{z - z_j}{z_i - z_j} \tag{10}$$

The collocation points z_i correspond to the so-called Chebyshev-Gauss-Lobatto points, which are defined in the interval [-1, 1] as:

$$\chi_i = \cos\left(\frac{2i - 1}{2(N - 1)}\pi\right), \quad i = 1...N - 1 \tag{11}$$

These Chebyshev points χ_i correspond with the roots of a Chebyshev polynomial of order N. A linear transformation is used for the nodes z_i on an arbitrary interval [a,b]:

$$z_i = \frac{b - a}{2}\chi_i + \frac{a + b}{2} \tag{12}$$

The second spatial derivative of the temperature at the i^{th} collocation points yields:

$$T_i'' = \sum_{i=1}^{N} L_i''(z_i)T_i \tag{13}$$

with L_i'' the second derivative in space of the Lagrange polynomial. The second spatial derivative at the collocation points **{T"}** can be calculated as follows:

$$\{\mathbf{T}''\} \approx [\mathbf{D}^2]\{\mathbf{T}\} \tag{14}$$

in which $[\mathbf{D}^2]$ is the Chebyshev collocation second-derivative matrix and **{T}** the temperatures at the collocation points. The Chebyshev collocation second-derivative matrix can be readily found in literature concerning spectral methods [16]. A backward Euler scheme is applied for the temporal discretization:

$$\frac{\partial T_i}{\partial t} \approx \frac{T_i^j - T_i^{j-1}}{\Delta t} \tag{15}$$

The superscripts j and j-1 denote the temperature at time t_j and t_{j-1}, respectively. Substituting in the partial differential heat equation yields:

$$\frac{\{\mathbf{T}^j\} - \{\mathbf{T}^{j-1}\}}{\Delta t} = \frac{k_z}{\rho c_p}[\mathbf{D}^2]\times\{\mathbf{T}^j\} \tag{16}$$

Rearranging gives the system of equations to be solved for the tape, substrate and coupled domain:

$$\left[\mathbf{I} - \Delta t\frac{k}{\rho c_p}[\mathbf{D}^2]^*\right]\times\{\mathbf{T}^j\} = \{\mathbf{T}^{j-1}\} \tag{17}$$

where **I** represents the identity matrix and the asterisk indicates that the boundary conditions as specified in Equation (6) and (7) are incorporated in the system matrix.

4 Results and discussion

The substrate and tape surface temperatures were calculated for two different cases using the developed optical and thermal model. Initially, the laser incident angle α was set at 22°, for which the incident heat flux distribution was shown in Figure 5. The graphs in Figure 5 show the substrate and tape surface temperature for two different placement velocities. It is evident that an increase in placement velocity, while keeping the laser power constant, results in a decrease of surface temperature. The surface temperature distribution follows the incident heat flux distribution. The substrate temperature decreases rapidly, due to conduction in the through-thickness direction, in the shadow of the compaction roller. The right graph in Figure 5 shows that the tape surface temperature increases rapidly and then cools down rather slowly. This is caused by the fact that the tape has a small thickness (~130 μm) and therefore is fully heated. Heat dissipation at the surface is therefore governed by the convective boundary conditions at both sides of the tape.

The rapid decrease in surface temperature on the substrate, as shown in Figure 5, suggests that an incident laser angle α of 22° is not optimal to heat the substrate. Reducing the angle α

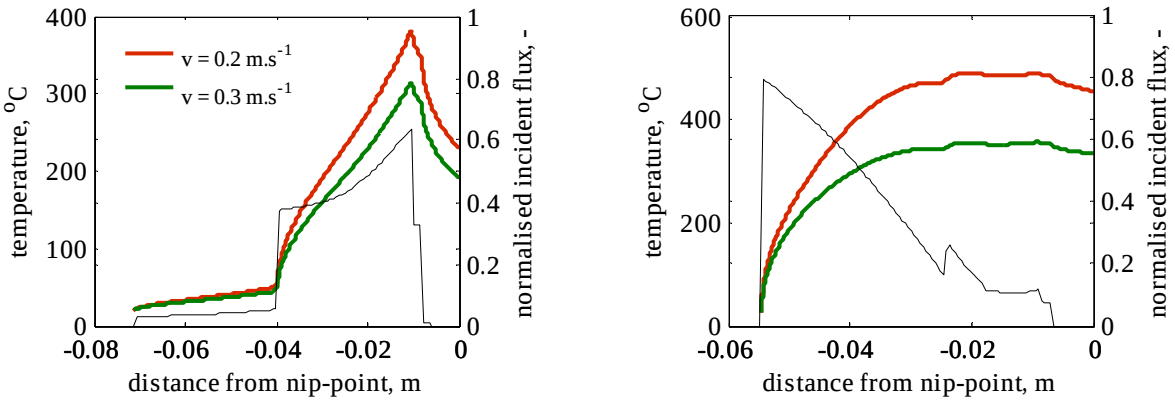

Figure 5 Incident laser angle α of 22° Left: substrate surface temperature for two different placement velocities. Right: Tape surface temperature. The thin black lines show the incident heat flux distribution.

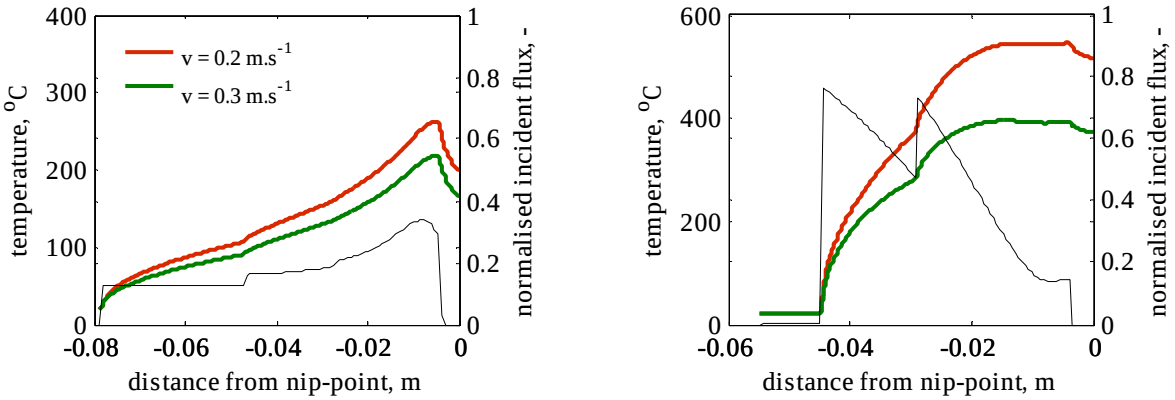

Figure 6 Incident laser angle α of 11° Left: substrate surface temperature for two different placement velocities. Right: Tape surface temperature. The thin black lines show the incident heat flux distribution.

reduces the shadow of the roller and might subsequently result in an increased surface temperature at the nip-point.

The left graph in Figure 6 shows the substrate temperature and normalised incident heat flux for a reduced laser angle α of 11°. The plotted incident heat flux (black line) indeed shows that the light is able to reach further down the nip-point. It is, however, also shown that the magnitude of the normalised incident heat flux has decreased compared to the case illustrated in Figure 5. The cause of this reduction is two-fold. In case the laser angle α decreases, the light is divided over a larger area. Furthermore, a larger portion of the light is reflected as the angle α decreases. The reflectivity R, using the refractive indices listed in Table 1, for an angle α of 22° equals approximately 0.15, compared to a value of 0.36 for an angle α of 11°. The reduced heat flux causes the substrate temperature to be significantly lower than the temperature obtained for a laser angle α of 22°.

The present analysis shows that the reflection of laser light should be taken into account when optimizing the laser assisted tape placement process. The optical properties of the tape and substrate are in this case important parameters. Currently, the refractive index was estimated to be in the range of most thermoplastics. Nevertheless, in order to improve the accuracy of the analysis, these should be obtained experimentally, taking into account the laser wavelength and relevant temperatures.

5 Conclusions and future work

A combined optical and thermal model is presented for the laser assisted tape placement process. A ray tracing procedure is adopted to calculate the incident laser heat flux distribution on the substrate and tape in the nip-point region. The calculated distribution is subsequently used in a one-dimensional transient thermal model to determine the substrate and tape temperatures. The analysis showed that decreasing the laser angle α, in order to reduce the shadowing effect of the compaction roller, not necessary means that the nip-point temperature increases. This is partly caused by the fact that the substrate reflectivity increases as the laser angle α is decreased.

Future work will focus on obtaining the relevant optical parameters experimentally, for the used materials, taking into account the laser wavelength and temperature range. Futhermore, a bond strength development and consolidation model will be added to the current thermal model. This will allow optimization of the process parameters for maximum part performance.

Acknowledgements

This research was funded by the EcoDesign Platform of the EU Clean Sky initiative. The support Advanced Fiber Placement Technology B.V. and Ten Cate Advanced Composites is gratefully acknowledged.

References

[1] Schledjewski, R.: Thermoplastic tape placement process – in situ consolidation is reachable. Plastic Rubber and Composites, **38**, 379-386 (2009)
[2] Lamontia, M.A. and Gruber, M.B.: Remaining developments required for commercializing in situ thermoplastic ATP. In: International SAMPE Symposium and Exhibition (Proceedings) 52, Baltimore (2007)
[3] Pitchumani, R. et al.: Analysis of transport phenomena governing interfacial bonding and void dynamics during thermoplastic tow-placement. Int. J. Heat Mass Transfer, **39**(9), 1883-1897 (1997)
[4] Sonmez, F.O. and Hahn, H.T.: Modeling of heat transfer and crystallization in thermoplastic composite tape placement process. Journal of Thermoplastic Composite Materials, **10**, 198-240 (1997)
[5] Thierney, J. and Gillespie Jr., J.W.: Modelling of heat transfer and void dynamics for the thermoplastic composite tow-placement process. Journal of Composite Materials, **37**(19), 1745-1768 (2003)
[6] Argawal, V. et al.: Thermal characterization of the laser-assisted consolidation process. Journal of Thermoplastic Composite Materials, **5**, 115-135 (1992)
[7] Thierney, J. and Gillespie Jr., J.W.: Modelling of in situ strength development for the thermoplastic tow placement process. Journal of Composite Materials, **40**, 1487-1506 (2006)
[8] Sonmez, F.O. et al.: Analysis of process induced residual stresses in tape placement. Journal of Thermoplastic Composite Materials, **15**, 525-544 (2010)
[9] Grove, S.M.: Thermal modeling of tape laying with continuous carbon fibre-reinforced thermoplastics. Composites, **19**, 367-375 (1988)
[10] Toso, Y.M.P. et al.: Thermal phenomena in fiber-reinforced thermoplastic tape winding process: Computational simulations and experimental validations. Journal of Composite Materials, **38**(2), 107-135 (2004)
[11] Hassan, N. et al.: A heat transfer analysis of the fiber placement composite manufacturing process. Journal of Reinforced Plastics and Composites, **24**(4), 867-888 (2007)
[12] Beyeler, E.P. and Güçeri, S.I.: Thermal analysis of laser-assisted thermoplastic-matrix composite tape consolidation. Journal of Heat Transfer, **110**(2), 424-430 (1988)
[13] Grove, S.M.: Thermal modeling of tape laying with continuous carbon fibre reinforced thermoplastic, **19**(5), 367-375 (1988)
[14] Seferis, J.C., Vilisaris, C.N.: Modelling – processing – structure relationships of polyetheretherketone (PEEK) based composites. In: 38th International SAMPE Symposium, p1236-1252 (1986)
[15] Cogswell, F.N.: Thermoplastic Aromatic Polymer Composites. Butterworth-Heinemann Ltd. (1992)
[16] Trefethen, L.: Spectral methods in MATLAB. Society for Industrial and Applied Mathematics, Philadelphia (2000)